Utilization of the Bias Momentum Approach for Capturing a Tumbling Satellite

Dimitar Nikolaev Dimitrov
Dept. of Aeronautics and Space Engineering
Tohoku University
Aoba01 Sendai 980-8579, Japan
Email: mitko@astro.mech.tohoku.ac.jp

Kazuya Yoshida
Dept. of Aeronautics and Space Engineering
Tohoku University
Aoba01 Sendai 980-8579, Japan
Email: yoshida@astro.mech.tohoku.ac.jp

***Abstract*— This paper deals with problems related to the capture of a tumbling satellite by a space robot. The minimization of the base attitude deviation after the contact with the target is discussed from the viewpoint of angular momentum distribution. A new capturing strategy utilizing bias momentum is introduced. By using the null space of the coupling inertia matrix we present a method for angular momentum redistribution while following a desired trajectory.**

I. Introduction

In recent years, capturing a free-floating object in orbit has been recognized as a priority task. Its solution is expected to be applied to a variety of space missions, involving servicing, inspection, and repairing operations. Furthermore the removal of space debris from orbit is a mission that should be taken very seriously. In order the realization of each task to be possible, a capturing operation should be performed.

Though capturing a tumbling object in space is a well known problem, it is very difficult to distinguish one of the solutions proposed up to now, which can solve it readily. Discussing the whole process from the trajectory planning to the post-impact control is an arduous task. The nature of the problems occurring in the different phases of the capture can be completely different so most of the researchers tend to separate the operation into approach, impact and post-impact motion.

In this paper we discuss a control strategy for capturing a tumbling satellite. Our main focus is the minimization of the base attitude deviation before and after the contact with the target. The concept of angular momentum management in a space manipulator is introduced. Furthermore we present such a momentum distribution that minimizes the base rotational motion.

Most of the solutions presented up to now are from viewpoint of the force impulse generated during the contact. Different strategies for its minimization are presented in [1] and [2]. The concept of joint resistance model was introduced in [3], furthermore the authors proposed the so called *impulse index* and *impulse ellipsoid* which adequately describe the force impulse characteristics. The effect of a "payload impact" on the dynamics of a flexible-link space robot is discussed in [4]. An impedance control, applied when capturing a non-cooperative target is proposed in [5]. The condition which guarantees that the target will not be pushed away after the contact is clarified. The application of the reaction null space approach in the approaching and post-impact phases is discussed in [6].

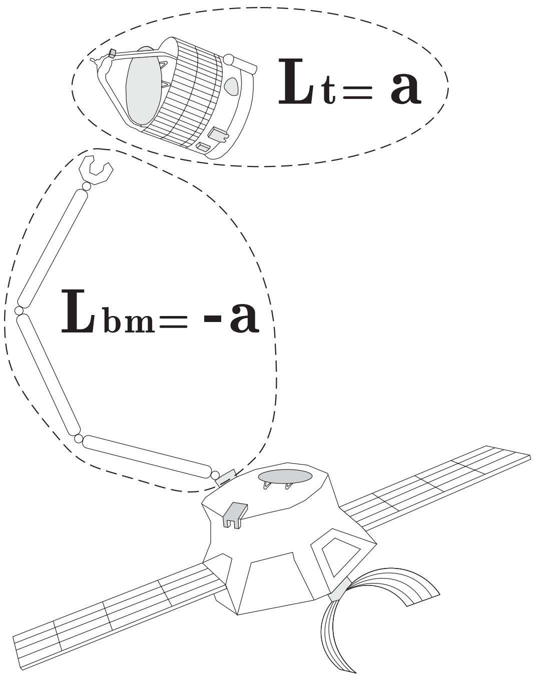

Fig. 1. Model of a space robot capturing a target, where $\boldsymbol{L}_{bm}$ denotes the coupling angular momentum between the manipulator arm and the base, and $\boldsymbol{L}_t$ stands for the angular momentum in the target satellite.

Another possible solution for the capturing problem is from the viewpoint of angular momentum. Grasping a target satellite without considering its momentum will impose difficulties for the post-impact control and most probably the capturing operation will fail. Different solutions are proposed up to now. One of them utilizes a device with controllable momentum wheels ("space leech"), which has to be attached to the target [7] and absorb the angular momentum. In [8] the idea of rotational motion-damper is proposed. Using *contact/push* based method the angular momentum from the target is transferred to the chaser satellite in portions. This could result however in separation from the target after each contact and therefore the usage of gas-jet thrusters for linear motion is unavoidable. This method might be useful if the amount of angular momentum in the target is very large and direct capture is impossible. A similar method using “impulsive control” is proposed by Yoshikawa et al. [9]. In [10] Nakamura et al. utilize a “tethered retriever” which is guided to the target through the tension force in the tether and thrusters positioned on the retriever. In the post-impact phase the angular momentum of the target is “absorbed” in attitude devices positioned on the retriever. In [11] the chaser satellite makes a fly around maneuver in such a way that the capturing operation can be conducted with small relative motion between the two systems. The authors propose a “free motion path method” which enables us to completely ignore the nonlinearity effect in the dynamics by taking advantage of the conservative quantities of the system.

Most of the methods cited above need information about the angular velocity and inertia parameters of the target satellite before the start of the approach. Such information is valuable for determining an optimal strategy. In [12] and [13] two solutions to this problem are presented. The results in both papers are based on successful experiments in orbit.

The force impulse generated during the contact is by all means an important factor for the attitude control, so we assume that one of the above stated minimization strategies can be utilized. Henceforth we will focus specifically on the influence of the pre-impact angular momentum distribution on the base attitude. The capturing strategy proposed in this paper is based on obtaining a favorable angular momentum distribution in the chaser satellite in order to facilitate the base attitude control in the post-impact phase. The main idea is to preload bias angular momentum in the chaser’s manipulator, which is with equal magnitude and opposite direction to the one in the target. Hence, after the capture the manipulator and target will have angular momentum equal to zero, see Fig. 1.

The paper is organized as follows. In section II we present the impact scenario and assumptions. Preliminaries and main notation are presented in section III. The angular momentum management task is discussed in section IV. Different pre-impact distributions are compared and angular momentum redistribution strategy is introduced. In section V the results of a numerical simulation are presented. Finally the conclusions are summarized in section VI.

II. Impact Scenario and Assumptions

In this study a serial-link manipulator mounted on a free-floating base is assumed to make contact with a target satellite. The target is rotating with a constant angular velocity and its angular momentum is known in advance. The contact model between the robot hand and the target is approximated with translational and rotational spring-damper system. For the sake of simplicity in this paper we do not assume a gripper attached to the end point of the manipulator. Hence the contact occurs just between two points. We assume that no gas-jet thrusters are used on the chaser’s base. For attitude stabilization only reaction wheels are utilized. A “soft approach” is considered, namely at the moment of the contact the relative velocity between the two contacting points is close to zero. That’s how we can minimize the force impulse, which if present could make the analysis much more complicated.

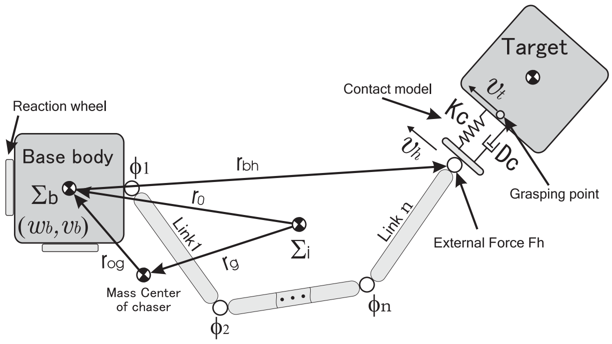

Fig. 2. Model of n DOF space robot capturing a target.

The following pre-impact strategy is then envisioned:

(1) estimate the motion trajectory of the target through data from visual and/or other sensors;

(2) determine the grasping point in inertial coordinates;

(3) design a desired trajectory to the grasping point such that at the moment of the catch the linear velocities of the two contacting points have almost the same magnitude and direction;

(4) during the approach to the target the angular momentum in the chaser satellite should be redistributed in such a way that the one in the manipulator has equal magnitude and opposite direction to the one in the target.

Obviously, such strategy implies that there is no relative linear velocity between the centroids of the chaser and the target. We assume that no external forces are present. Therefore the momentum of the entire system will be conserved during all the three phases of the capturing operation.

III. Preliminaries and Main Notation

We assume a serial n link manipulator and a system of reaction wheels attached to a floating base as shown in Fig. 2. The points Σ_i and Σ_b denote the origin of the inertial frame and the base centroid, respectively. The linear and angular velocity of the satellite base $(\boldsymbol{v}_b, \boldsymbol{\omega}_b)$ and the motion rates of the joints $(\dot{\boldsymbol{\phi}})$ are chosen as generalized coordinates. $\boldsymbol{v}_h$ and $\boldsymbol{\omega}_h$ are the linear and angular velocities of the end-effector. The behavior of a free-floating manipulator system can be fully described by the momentum conservation equation:

$$\begin{bmatrix} \boldsymbol{P} \\ \boldsymbol{L} \end{bmatrix} = \boldsymbol{H}_b \begin{bmatrix} \boldsymbol{v}_b \\ \boldsymbol{\omega}_b \end{bmatrix} + \boldsymbol{H}_{ac} \begin{bmatrix} \dot{\boldsymbol{\phi}}_m \\ \dot{\boldsymbol{\phi}}_r \end{bmatrix} + \begin{bmatrix} \boldsymbol{O} \\ \boldsymbol{r}_0 \times \boldsymbol{P} \end{bmatrix} \quad (1)$$

The inertia matrices are expressed as follows:

$$\boldsymbol{H}_b = \begin{bmatrix} w\boldsymbol{E} & w\hat{\boldsymbol{r}}_{og}^T \\ w\hat{\boldsymbol{r}}_{og} & \boldsymbol{H}_\omega \end{bmatrix} \in R^{6\times6}$$

$$\boldsymbol{H}_{ac} = \begin{bmatrix} \boldsymbol{H}_{bm} \; \boldsymbol{H}_{br} \end{bmatrix} = \begin{bmatrix} \boldsymbol{J}_{tg} \\ \boldsymbol{H}_{\omega\phi} \end{bmatrix} \in R^{6\times n}$$

where w, $\boldsymbol{E} \in R^{3\times3}$ and $\boldsymbol{O} \in R^{3\times3}$ stands for the total mass of the chaser satellite, the identity matrix and the null matrix, respectively. $\boldsymbol{r}_0$ and $\boldsymbol{r}_{og}$ are distances as depicted in Fig. 2. $\boldsymbol{P}$ and $\boldsymbol{L}$ are the linear and angular momentum of the chaser satellite. The $(\cdot)^T$ and $\hat{(\cdot)}$ operators denote a matrix transpose and a skew-symmetric representation of a three dimensional vector. Expressions for $\boldsymbol{H}_\omega$, $\boldsymbol{J}_{tg}$ and $\boldsymbol{H}_{\omega\phi}$ can be found in [14].

The matrix $\boldsymbol{H}_b$ is the base inertia, $\boldsymbol{H}_{bm}$ and $\boldsymbol{H}_{br}$ are the coupling inertia matrices between the base and manipulator, and the base and reaction wheels, respectively. The three matrices are functions of the joint and base variables. However if we assume that no external forces act on the chaser satellite, $\boldsymbol{H}_b$, $\boldsymbol{H}_{bm}$ and $\boldsymbol{H}_{br}$ will be just a function of $\boldsymbol{\phi}$. This fact is very useful, because with a proper joint control, one can ensure a minimal base attitude deviation while making a desired approach to the target. Realization of such a behavior can be obtained by using the *reaction null space* approach. It will be outlined in the next sub-section.

The angular momentum component of equation (1) is of special interest to us, because it is directly related to the base rotational motion. Attitude destabilization is mostly undesirable, because it can lead to various problems. In order to emphasize on the base attitude, we can cancel out $\boldsymbol{v}_b$ from (1) to obtain:

$$\boldsymbol{L} = \tilde{\boldsymbol{H}}_b\boldsymbol{\omega}_b + \tilde{\boldsymbol{H}}_{bm}\dot{\boldsymbol{\phi}}_m + \tilde{\boldsymbol{H}}_{br}\dot{\boldsymbol{\phi}}_r \tag{2}$$

where $\tilde{\boldsymbol{H}}_{ac} = \left[\ \tilde{\boldsymbol{H}}_{bm}\ \tilde{\boldsymbol{H}}_{br}\ \right] = \boldsymbol{H}_{\omega\phi} - \hat{\boldsymbol{r}}_{og}\boldsymbol{J}_{tg} \in R^{3\times n}$, $\tilde{\boldsymbol{H}}_b = \boldsymbol{H}_\omega - w\hat{\boldsymbol{r}}_{og}\hat{\boldsymbol{r}}_{og}^T \in R^{3\times 3}$ and $\boldsymbol{P} = 0$ is assumed. Each of the three components on the right side of equation (2) defines a partial angular momentum of the system. The first term represents the angular momentum of the base body as a result of its attitude change, the second is related to the manipulator motion and is called the coupling angular momentum between the base and the manipulator. The third term is the coupling angular momentum between the reaction wheels and the base.

$$\boldsymbol{L}_b = \tilde{\boldsymbol{H}}_b\boldsymbol{\omega}_b \ \ ; \ \ \boldsymbol{L}_{bm} = \tilde{\boldsymbol{H}}_{bm}\dot{\boldsymbol{\phi}}_m \ \ ; \ \ \boldsymbol{L}_{br} = \tilde{\boldsymbol{H}}_{br}\dot{\boldsymbol{\phi}}_r$$

By applying internal torques in the joints, the three partial angular momentums can change in a desired way. We call this change momentum redistribution. In other words though the amount of $\boldsymbol{L}$ present in the system is constant, its distribution over the base, manipulator and reaction wheels can vary. Our aim in this paper is to show that the momentum distribution before the contact with the target is closely connected to the base attitude deviation after the contact. With a proper choice of the three partial angular momentums one can facilitate the post-impact attitude control.

A. The Null Space Approach

In this section and for the rest of the article we assume that a kinematical redundancy with respect to the base motion task is present. In other words we require the number of joints (n) to be larger than the number of base variables (m). Recall the note we made on the significance of satellite-base attitude. Now we will formulate the reaction null space with respect to the base attitude only (this technique is also called "selective reaction null-space").

Solving equation (2) for the joint velocity rates, one obtains:

$$\dot{\boldsymbol{\phi}}_m = \tilde{\boldsymbol{H}}_{bm}^{+}(\boldsymbol{L} - \tilde{\boldsymbol{H}}_{br}\dot{\boldsymbol{\phi}}_r) + \boldsymbol{P}_{RNS}\dot{\boldsymbol{\zeta}} \tag{3}$$

where $\boldsymbol{P}_{RNS} = (\boldsymbol{E}_n - \tilde{\boldsymbol{H}}_{bm}^{+}\tilde{\boldsymbol{H}}_{bm})$ is the projector onto the null space of $\tilde{\boldsymbol{H}}_{bm}$, $\dot{\boldsymbol{\zeta}} \in R^n$ is an arbitrary vector, $(\cdot)^+$ operator denotes the pseudo inverse of a matrix (Moore-Penrose generalized inverse) and $\boldsymbol{E}_n \in R^{n\times n}$ is the identity matrix. $\boldsymbol{P}_{RNS}$ exists if the manipulator is redundant in the sense explained above. If the joint velocities are obtained from the second part of equation (3), they will not affect the angular momentum distribution and the base attitude whatsoever. We will utilize this property in the following sections. For a substantial discussion on the reaction null space approach, see [6], [15].

IV. Angular Momentum Distribution

One of the main characteristics of a capturing operation in orbit is the momentum conservation if there are no external forces. If just the chaser or target system is considered, it might undergo a momentum change, but in the entire system the momentum will be preserved. This is valid for the approach, impact and post-impact phases. In this section we divide the entire system into four components and discuss the capturing operation from viewpoint of the angular momentum stored in them, see Fig. 3.

During the approaching phase the chaser robot can change its configuration in a desired way in order to grasp a predefined point of the target satellite. According to the optimization task we want to perform, the configuration change can be different. Recall that our main concern is keeping the base attitude deviation close to zero before, during and after the contact. Hence the constraint $\boldsymbol{\omega}_b = 0$ should be imposed. Additional constraints will be imposed from the trajectory that should be followed while the desired angular momentum distribution is obtained. In the next sub-sections we compare four such distributions. In order to make contrast between the four cases depicted in Fig. 3, the manipulator joints will be servo blocked after the contact, and a simple PD feedback attitude control will be utilized. In this paper we assume that the capturing operation is successfully complete when the base body, manipulator system and the target become stationary.

A. Non-Bias Distribution

The first candidate for a possible distribution, is depicted in Fig. 3 (**Case A**). In this paper we call this case "non-bias" because at the end of the approaching phase $\boldsymbol{L}_{bm} = 0$. After the contact $\boldsymbol{L}_t$ distributes over the entire system. How fast it will be transferred to the base depends on factors like: pre-impact configuration, force impulse that occurs during the impact phase, post-impact control. Note that though our post-impact control is just blocking the joints, the whole angular momentum will not necessarily be transferred directly to the base body. Some part of it will stay in the target, other will be distributed over the links.

Because of the constraint $\boldsymbol{\omega}_b = 0$, the attitude stabilization devices will work to compensate the base deviation. In this paper we consider a class of reaction wheels used in ETS-VII - max. torque of 0.1 Nm and capacity of 16 Nms. As a result of the maximum torque restriction the reaction wheels will not manage to accommodate the angular momentum transferred to the base in a short time. Hence a base rotational motion will occur. The numerical simulation in section V, will show that the momentum distribution in **Case A** yields a big attitude deviation.

B. Angular Momentum in the Reaction Wheels

Now let us suppose that at the start of the capturing operation we have already stored angular momentum in the reaction wheels and its magnitude is equal and with opposite sign to the one in the target, see Fig. 3 (**Case B**). In this case the momentum of the entire system at the end of the approaching phase is equal to zero, but the accommodation rate of $\boldsymbol{L}_t$ will be the same as in the non-bias case. When the capturing operation comes to an end, in **Case B** the reaction wheels will be stationary, while in the non-bias case they were loaded with the momentum from the target. However, from the viewpoint of base attitude no optimization is done.

The reason for such a behavior is that the angular momentum, like an electrical charge, cannot "jump" from one place to another if there is no "connection". In both cases the "connection" is the base of the chaser, but the capacity of this connection is limited, and equal amount of angular momentum can go through. The limitation is determined by two restrictions, namely $\boldsymbol{\omega}_b = 0$, and the torque limitation of the reaction wheels. Hence the rate of momentum accommodation from the target will be the same if at the start of the post-impact phase $\boldsymbol{L}_{br} = 0$ or $\boldsymbol{L}_{br} \neq 0$. The only exception can occur when $\boldsymbol{L}_t + \boldsymbol{L}_{br} > \boldsymbol{L}_{br}^{max}$ (where $\boldsymbol{L}_{br}^{max}$ is the maximum amount of angular momentum that can be stored in the attitude stabilization devices), then one will not be able to accommodate $\boldsymbol{L}_t$ in the reaction wheels.

C. Bias Angular Momentum in the Manipulator

The main difference between **Case B** and **Case C** in Fig. 3 is that the momentum is stored either in $\boldsymbol{L}_{br}$ or in $\boldsymbol{L}_{bm}$. These two distributions however, lead to different results from the viewpoint of base attitude deviation.

The distribution in **Case C** provides us with different options. One of them is again using the reaction wheels as a buffer for angular momentum. The other however, utilizes the fact that after the contact $\boldsymbol{L}_t$ "entering" the chaser could be canceled out with the one preloaded in $\boldsymbol{L}_{bm}$. Therefore in the post-impact phase just the remaining amount of angular momentum in the base, manipulator and target should be redistributed in order the system to come to a complete stop. Since in this case the angular momentum that needs to be distributed is actually zero even blocking

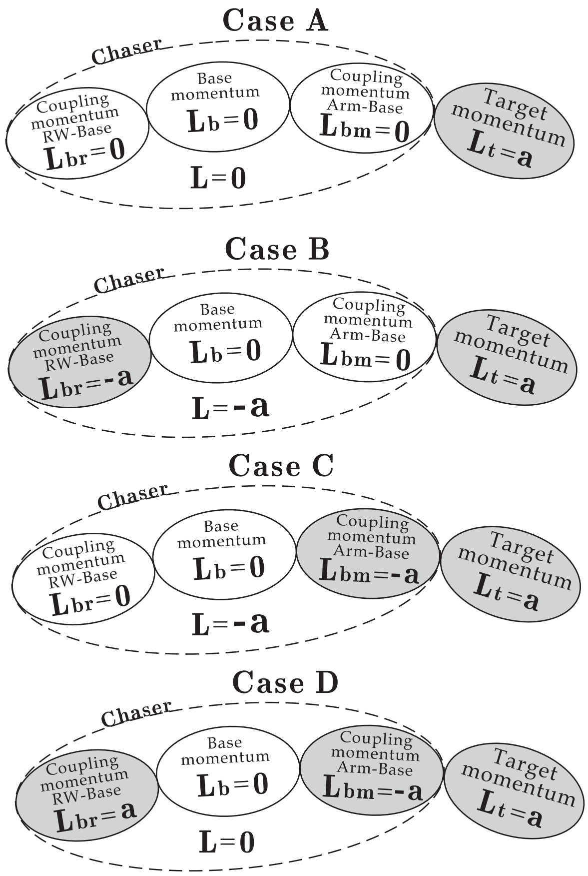

Fig. 3. Four cases of pre-impact angular momentum distribution, where **A** and **B** are non-bias cases and in **C** and **D** the bias momentum approach is utilized.

the manipulator joints will lead to a successful completion of the capturing operation. We should note however that if in **Case C** no post-impact control is applied, base attitude deviation might occur as a result of the impact force generated during the contact.

Recall that we imposed constraints just over the base attitude. Therefore in the approaching phase the manipulator motion will result in a change of the base translational motion. However it is possible to move the arm in such a way that no base motion occurs whatsoever. Therefore two alternatives for loading bias angular momentum can be outlined (keep in mind that the constraint $\boldsymbol{\omega}_b = 0$ is assumed):

(a) all the angular momentum is in the manipulator;
(b) one part of the angular momentum is stored in the manipulator, the remaining in the translation of the base, which is caused by the arm motion.

Note that the latter option is precisely the physical equivalent of the coupling angular momentum between the manipulator and the base. In the post-impact phase there is no difference between options (a) and (b), because in both cases the angular momentum can be utilized immediately for canceling out $\boldsymbol{L}_t$. In the approach to the target however, the realization of option (a) is much more difficult task. Two reasons could be outlined:

- three additional constraints for the base linear motion should be imposed;

- if all the angular momentum is to be stored in the robot arm its links should have large inertia or the manipulator should have additional redundancy.

The distribution in option (b) is the better of the two because from the bias momentum strategy point of view there is no drawback, and imposing three additional constraints for the base linear motion is avoided.

D. Angular Momentum Management

In this sub-section the problem of loading desired amount of angular momentum in the base and manipulator arm while following a predefined trajectory is discussed. We will utilize the differential kinematics equation of a free floating manipulator.

$$\begin{bmatrix} \boldsymbol{v}_h \\ \boldsymbol{\omega}_h \end{bmatrix} = \boldsymbol{J}_m \dot{\boldsymbol{\phi}}_m + \boldsymbol{J}_b \begin{bmatrix} \boldsymbol{v}_b \\ \boldsymbol{\omega}_b \end{bmatrix} \tag{4}$$

where $\boldsymbol{J}_b$ and $\boldsymbol{J}_m$ are the base and manipulator Jacobian matrices. We start the derivation by observing from (4) that each of the two equations is a good candidate for a motion constraint. In the derivation we consider both of them, however for following a desired trajectory just the first one could be sufficient. Combining (4) with (2) and solving for $\dot{\boldsymbol{\phi}}_m$ we obtain:

$$\dot{\boldsymbol{\phi}} = \boldsymbol{G}^{+} \begin{bmatrix} \boldsymbol{L} - \tilde{\boldsymbol{H}}_{br}\dot{\boldsymbol{\phi}}_r \\ \dot{\boldsymbol{x}}_h - \boldsymbol{J}_b \dot{\boldsymbol{x}}_b \end{bmatrix} + \boldsymbol{P}_G \dot{\boldsymbol{\zeta}} \tag{5}$$

where $\boldsymbol{G} = \begin{bmatrix} \tilde{\boldsymbol{H}}_{bm}^T & \boldsymbol{J}_m^T \end{bmatrix}^T$ and $\boldsymbol{P}_G = \boldsymbol{E}_n - \boldsymbol{G}^{+}\boldsymbol{G}$. $\dot{\boldsymbol{x}}_h = \begin{bmatrix} \boldsymbol{v}_h^T \ \boldsymbol{\omega}_h^T \end{bmatrix}^T$ and $\dot{\boldsymbol{x}}_b = \begin{bmatrix} \boldsymbol{v}_b^T \ \boldsymbol{\omega}_b^T \end{bmatrix}^T$. Again $\boldsymbol{\omega}_b = 0$ was assumed. The condition for existence of $\boldsymbol{P}_G$ is somewhat different from the one made about $\boldsymbol{P}_{RNS}$ in sub-section III-A. In order $\boldsymbol{P}_G$ to be different from zero $n > m_{task}$ must be satisfied (m_{task} are all the task variables, not just the base ones). The null space component in (5) is an intersection between the null space of $\tilde{\boldsymbol{H}}_{bm}$ and the one of $\boldsymbol{J}_m$, therefore it does not affect neither the trajectory of the end effector, nor the base attitude subtask (this is called “self-motion”). Hence $\boldsymbol{P}_G$ can be utilized for realization of optimization tasks such as joint velocity minimization.

As we noted in sub-section IV-B the amount of $\boldsymbol{L}_{br}$ does not affect the rate of angular momentum redistribution. Therefore the accommodation of $\boldsymbol{L}_t$ during the post-impact phase does not depend on the angular momentum already stored in the reaction wheels. We can utilize this fact in order to obtain a distribution as depicted in Fig. 3 (**Case D**). In this case $\boldsymbol{L} = 0$, however it is considered as a favorable distribution, since $\boldsymbol{L}_{bm} = -\boldsymbol{L}_t$. We want to point out that even without using external torques the bias momentum approach can be applied successfully, through synchronized motion between the manipulator arm and the reaction wheels during the approaching phase. Distribution as depicted in **Case D** can be obtained by utilizing equation (5).

Since we assumed that $\boldsymbol{L}$ is constant during the approach, the only term in (5) that can change the momentum distribution is $\tilde{\boldsymbol{H}}_{br}\dot{\boldsymbol{\phi}}_r$ (note that the null space component

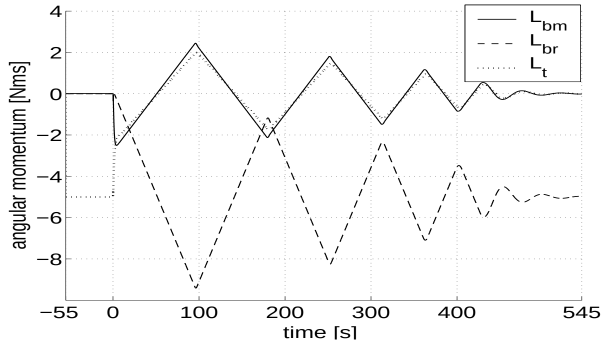

Fig. 4. Angular momentum distribution for **Case A**.

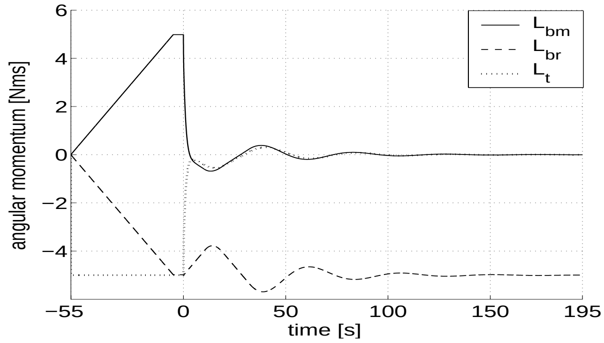

Fig. 5. Angular momentum distribution for the bias case (**Case D**).

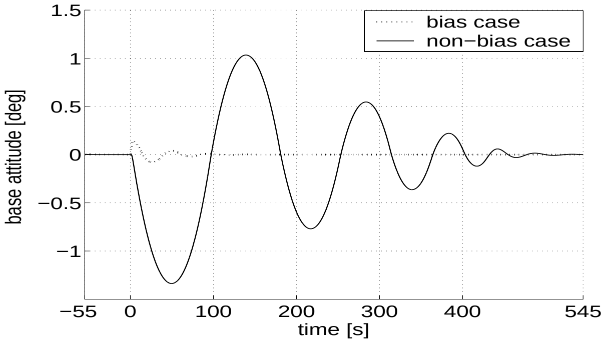

Fig. 6. Base attitude deviation comparison between the bias and the non-bias cases.

$\boldsymbol{P}_G\dot{\boldsymbol{\zeta}}$ will not contribute to the momentum of the system whatsoever). Applying a feed forward torque in the joints of the reaction wheels, will result in such a manipulator motion that the rate of change of $\boldsymbol{L}_{bm}$ will be equal to the one of -$\boldsymbol{L}_{br}$. Therefore by controlling the torque input in the joints of the reaction wheels, one can obtain a desired angular momentum distribution in the chaser system.

One obvious difference between **Case D** and the non-bias case is that in the latter one, the whole angular momentum has to be accommodated for a very short time after the contact with the target, if zero base attitude change is desired. If the bias momentum approach is utilized however, there is enough time for loading $\boldsymbol{L}_{bm}$ while following the desired trajectory and it can be done without any change of the base rotational motion.

V. Simulation Study

In this section we present the results from a numerical simulation of a 3 DOF planar manipulator capturing a target satellite. The parameters of the chaser and the target are shown in Table 1.

TABLE I
MODEL PARAMETERS

	base	target	link1	link2	link3	RW
$\boldsymbol{m}$ [kg]	1000	300	100	100	100	10
$\boldsymbol{l}$ [m]	1.0x1.0	1.0x1.0	1.0	1.0	1.0	-
$\boldsymbol{I}$ [kgm^2]	1250	219	33	33	33	0.45

Figures 4 and 5 depict a comparison between $\mathbf{Case\ A}$ (non-bias) and $\mathbf{Case\ D}$ (bias) from the viewpoint of angular momentum. At the start of the simulation $\boldsymbol{L}_t = -5$ Nms. The inertial frame is chosen to coincide with the mass center of the entire system. The contact with the target occurs at $t = 0$ sec. As already explained the joints are blocked with high differential gain after the contact, and in the post-impact phase a reaction wheel is utilized for minimization of the base attitude through a PD feedback control. In both cases equal gains are used, and at the end of the capture the angular momentum is stored in the reaction wheel.

As we noted in section IV-D, a desired angular momentum distribution can be successfully obtained if the motion of the manipulator and reaction wheels is synchronized. Before the start of the capturing operation, the desired trajectory of the end-effector as well as the angular momentum distribution that should be obtained, will be determined. Hence one can use a feed forward torque method for controlling the reaction wheels during the approaching phase. In the simulation where bias momentum approach is adopted, during the first 50 sec. -0.1 Nm torque is applied on the attitude stabilization device. Hence loading the base plus manipulator with $\boldsymbol{L}_{bm} = 5$ Nms. After $\boldsymbol{L}_{bm}$ becomes with equal magnitude and different sign compared to $\boldsymbol{L}_t$ and before the contact with the target, the chaser system continues its motion in such a way that no angular momentum is redistributed between the reaction wheel and $\boldsymbol{L}_{bm}$. Resembling motion can be observed during the entire approaching phase in the non-bias case.

In the post-impact phase the reaction wheel has to minimize the base attitude, and simultaneously accommodate the momentum from the target. Since the base attitude control is the priority task, the reaction wheel is working in response to the attitude error. Also because the control torque is saturated at 0.1 Nm, the profile of $\boldsymbol{L}_{br}$ has a constant slope in Fig. 4. Associated with this profile, the angular momentum in the base and manipulator system is repeatedly exchanged with the reaction wheel. This undesired effect can be minimized if bias momentum approach is utilized during th approach to the target. The base attitude history in both cases is given in Fig. 6. The difference in the two profiles shows what is the influence of the angular momentum of the target over the base rotational motion of the chaser satellite in the post-impact phase.

Some limitations do exist however. Even if the base linear motion is utilized, still loading a large amount of angular momentum in the manipulator presumes that either it has some additional redundancy, or the links have large inertia. Otherwise the robot arm would have to move with high velocities. The bias approach does not give all the solutions to a capturing operation, but if utilized it can facilitate the post-impact control. Even if just a part of the target's angular momentum is loaded with opposite sign in the base plus manipulator system, improved results from the viewpoint of base attitude could be obtained.

VI. CONCLUSIONS

In this paper, a new strategy for capturing a free-floating satellite initially loaded with angular momentum was presented. We focused on the momentum distribution in the chaser satellite during the approaching and post-impact phases. The idea of preloading bias angular momentum in the chaser's base and manipulator arm was discussed. The entire system consisted of chaser and target satellites, was divided into four parts and different pre-impact momentum distributions were compared. The validity of the strategy proposed in this paper was verified by a numerical simulation.

REFERENCES

[1] K. Yoshida, R. Kurazume, "Modeling of collision dynamics for space free-floating links with extended generalized inertia tensor," *Proc. 1992 IEEE Int. Conf. Robot. Automat.,* Nice, France, pp. 899-904, May, 1992.

[2] L. B. Wee, M. W. Walker, "On the dynamics of contact between space robots and configuration control for impact minimization," *IEEE Trans. Robot. Automat.,* vol. 9, pp. 581-591, Oct. 1999.

[3] K. Yoshida, N. Sashida, "Modeling of impact dynamics and impulse minimization for space robots," *Proc. 1993 IEEE/RSJ Int. Conf. Intell. Robots Syst. (IROS'93),* Yokohama, Japan, pp. 2064-2069, July 1993.

[4] X. Cyril, G. J. Jaar, and A. K. Misra, "The effect of payload impact on the dynamics of a space robot," *Proc. 1993 IEEE/RSJ Int. Conf. Intell. Robots Syst. (IROS'93),* Yokohama, Japan, pp. 2070-2075, 1993.

[5] K. Yoshida, H. Nakanishi, et al., "Dynamics, control and impedance matching for robotic capture of a non-cooperative satellite," *Advanced Robotics,* vol. 2, no. 2, pp. 175-198, 2004.

[6] D. N. Nenchev, K. Yoshida, "Impact analysis and post-impact motion control issues of a free-floating space robot subject to a force impulse," *IEEE Trans. Robot. Automat.,* vol. 15, no. 3, pp. 548-557, June 1999.

[7] M. W. Walker, D. M. Kim, "Satellite stabilization using space leeches," *Proc. IEEE Amer. Contr. Conf.,* San Diego, CA, May 23-25, 1990, pp. 1314-1319.

[8] S. Matunaga, T. Kanzawa, Y. Ohkami "Rotational motion-damper for the capture of an uncontrolled floating satellite ," *Cont. Eng. Practice,* vol. 9, pp. 199-205, 2001.

[9] S. Yoshikawa, K. Yamada, "Impulsive control for angular momentum management of tumbling spacecraft," *24th ISTS,* Miyazaki, Japan, May 30 - June 6, 2004.

[10] Y. Nakamura, F. Sasaki, S. Nakasuka, "Guidance and control of "Tethered retriever" for future on-orbit service missions," *24th ISTS,* Miyazaki, Japan, May 30 - June 6, 2004.

[11] Y. Tsuda, S. Nakasuka, "New attitude motion following control algorithm for capturing tumbling object in space," *Acta Astronautica,* vol. 53, pp. 847-861, 2003.

[12] H. Kamimura, S. Kowamoto, S. Nishida, et al., "Detection and motion estimation of small target using color image processing," *24th ISTS,* Miyazaki, Japan, May 30 - June 6, 2004.

[13] S. Nakasuka, R. Funase, S. Kimura, et al., "Micro-LABSAT experiment of target motion estimation and tracking for future on-orbit service missions," *24th ISTS,* Miyazaki, Japan, May 30 - June 6, 2004.

[14] K. Yoshida, "Practical coordination control between satellite attitude and manipulator reaction dynamics based on computed momentum concept," *Proc. 1994 IEEE/RSJ/GI Int. Conf. Intell. Robots Syst. (IROS'94),* Munich, Germany, pp. 1578-1585, Sep. 1994.

[15] D. N. Nenchev, K. Yoshida, "Reaction Null-Space Control of Flexible Structure Mounted Manipulator Systems," *IEEE Trans. Robot. Automat.,* vol. 15, no. 6, pp. 1011-1023, Dec. 1999.